agriculture

MDPI

Article

Impact of Salinity, Elevated Temperature, and Their Interaction with the Photosynthetic Efficiency of Halophyte Crop *Chenopodium quinoa* Willd

Elena Shuyskaya *, Zulfira Rakhmankulova, Maria Prokofieva, Varvara Kazantseva and Nina Lunkova

K.A. Timiryazev Institute of Plant Physiology, Russian Academy of Science, 127276 Moscow, Russia; zulfirar@mail.ru (Z.R.); maria.vdovitchenko@gmail.com (M.P.); vkazantceva90@gmail.com (V.K.); nina.lunkova@gmail.com (N.L.)

* Correspondence: evshuya@gmail.com

Abstract: *Chenopodium quinoa* is a genetically diverse crop that can adapt to a wide range of environments, including temperatures and salinities. However, only a few studies have assessed the combined effects of two or more environmental factors on *C. quinoa*. Here, we investigated the effects of salinity (300 mM NaCl), elevated temperature (35 °C), and their interaction with growth, water–salt balance, the efficiency of photosystem II (PSII), the activity of cyclic electron transport (CET) around photosystem I (PSI), Rubisco and PEPC enzyme content, and the expression of photosynthetic genes. We found that elevated temperature did not decrease the biomass but caused a significant increase in the water and potassium content of *C. quinoa* leaves. The decrease in PSII efficiency under elevated temperature was accompanied by an increase in the expression of genes encoding the components of PSII (*psbA*) and linear electron transport (*FDI*), as well as the main photosynthetic protein Rubisco (*rbcL*). Moreover, the strongest effect was induced by the combined effect of elevated temperature and salinity, which induced high oxidative stress (a threefold increase in MDA), a threefold decrease in the biomass, a twofold decrease in PSII efficiency, and a two- to eightfold decrease in the expression of the photosynthetic genes *psbA*, *FDI*, and *rbcL*. PSI was more tolerant to all forms of stress; however, the combined effect of elevated temperature and salinity downregulated the expression of *PGR5* and *FNR1*, which may diminish the role of PGR5/PGRL1-dependent CET in favor of the NDH-dependent CET of PSI. The obtained data on the functioning of photosystems and the expression of photosynthetic genes under combined stress (elevated temperature and salinity) can make a significant contribution to understanding the mechanisms of tolerance of *C. quinoa* to multiple stresses under climate change conditions.

Keywords: combined stress; photosystems I and II; cyclic electron transport; PGR5/PGRL1-dependent pathway; NDH-dependent pathway; Rubisco

Citation: Shuyskaya, E.; Rakhmankulova, Z.; Prokofieva, M.; Kazantseva, V.; Lunkova, N. Impact of Salinity, Elevated Temperature, and Their Interaction with the Photosynthetic Efficiency of Halophyte Crop *Chenopodium quinoa* Willd. *Agriculture* **2023**, *13*, 1198. https://doi.org/10.3390/agriculture13061198

Academic Editor: Matevz Likar

Received: 6 May 2023
Revised: 29 May 2023
Accepted: 2 June 2023
Published: 4 June 2023

1. Introduction

Soil salinity is one of the main abiotic stresses that negatively affect crop yields around the world [1]. Salt stress affects over 1 billion hectares of land and over 50% of irrigated agricultural land [1,2]. Salinity retards the growth, development, and productivity of plants due to ion stress and accompanying oxidative stress [3]. In addition, salinity increases the impact of soil drought on plants by adding the osmotic pressures, which are further intensified by the effects of elevated temperatures and irregular rainfall [1]. Increasing global warming in recent decades has contributed to an increase in the frequency and duration of exposure to high temperatures on crops, thereby posing a serious threat to agriculture [4]. Elevated temperatures can disrupt plant growth and development, resulting in reduced productive potential and serious crop losses [5].

Chenopodium quinoa is a halophyte crop widely cultivated for the excellent nutritional value of the seeds [3,6,7]. The Food and Agriculture Organization has recommended *C.*

quinoa as a key crop for dry and saline regions [6]. The effects of salinity and drought on *C. quinoa* are well studied, whereas only a few studies have examined the effects of other types of stress, including heat, cold, or UV-B radiation. Moreover, even fewer studies have examined the combined effect of two or more factors that commonly co-occur under natural conditions [6,8,9].

Large differences in salt tolerance between *C. quinoa* cultivars have been revealed by agronomic and physiological analyses [3,8,10,11]. For example, some *C. quinoa* cultivars can tolerate salinity up to 750 mM NaCl [12]. The main mechanisms involved in salt tolerance in *C. quinoa* include osmotic regulation via the accumulation of inorganic ions (i.e., Na^+, K^+ and Cl^-) that can effectively control Na^+ sequestration in vacuoles and epidermal bladder cells (EBCs); reduced stomatal density to facilitate more efficient water use; and high resistance to reactive oxygen species (ROS) [3,13,14]. EBCs play an important role in sodium sequestration, improve K^+ retention, and store metabolites that help modulate ion ratios in *C. quinoa* [8]. The mechanisms by which salt tolerance relates to the photosynthetic activity of *C. quinoa* remain poorly understood [13,15,16]. A well-known effect of salinity is the decrease in CO_2 assimilation and is associated primarily with stomatal conductance limitations [16,17]. It has also been shown that high salinity (300 mM NaCl) can lead to structural disorders of chloroplasts and decreased F_m and F_v/F_m [13], as well as to increased nonphotochemical quenching (NPQ) of energy [18]. This in turn can lead to the suppression of PSII effectivity in *C. quinoa*. In addition, ionic toxicity can affect the activity of photosynthetic enzymes and promote the degradation of pigment protein complexes in the thylakoid membranes of *C. quinoa* [16,18].

Elevated temperatures are a major form of abiotic stress that may become more common due to climate change. Elevated temperature limits plant productivity since the main elements of photosynthesis are heat-sensitive and are inhibited under elevated temperature [19]. Moreover, Calvin cycle reactions and photosynthetic electron transport, primarily that of photosystem complex II (PSII), are the most susceptible to high temperature [19–21]. Disruption of the photosynthetic apparatus leads to ROS formation, such as singlet oxygen in PSII and superoxide radicals in PSI, among others. Moderately high temperatures do not direct damage PSII but do so indirectly by promoting the production of ROS [19]. High temperatures damage PSII by blocking linear electron transport (LET), which reduces the supply of energy to chloroplasts. In this case, cyclic electron transport (CET) around PSI combines with cyclic photophosphorylation to stimulate ATP synthesis, thereby helping plants withstand stress [22]. Moreover, CET is thought to have two main functions: to provide ATP for the Calvin cycle and to help maintain the proton gradient (ΔpH) that underlies NPQ for PSII photoprotection [23,24]. PSI is usually more stable than PSII [23], and CET plays an important role in protecting PSI from heat stress [19,25]. It is known that CET includes two pathways: a chloroplast NADH dehydrogenase-like complex-dependent pathway and a PGR5/PGRL1 protein-dependent pathway [26–29]. Moreover, the PGR5/PGRL1-dependent CET is the major pathway for plants with C_3 photosynthesis [29]. PGR5/PGRL1-dependent CET plays an important role in plant responses to abiotic stress [24,30], as it protects PSII and PSI from photooxidative damage via ΔpH formation, maintains the integrity of the thylakoid membrane, and facilitates normal expression of genes of the main components of the photosystem [24]. Furthermore, NDH-dependent CET may be involved in plant responses to various environmental stresses, including high temperature stress [29,31]. The most sensitive step of the Calvin cycle appears to be the activation of Rubisco by Rubisco-activase, and the Rubisco enzyme is considered to be relatively thermostable [19]. Elevated temperatures can reduce the expression of Rubisco genes (*rbcL* and *rbcS*); however, differences in heat tolerance of Rubisco synthesis have been shown both between species and within the same species [20]. In addition, plants can use Rubisco as a reserve of nitrogen/amino acids, and it is therefore excreted from chloroplasts and stored in vacuoles. Under stress conditions, Rubisco is actively cleaved by proteases and sent to other organs to support protein synthesis [32,33]. During stress, the phosphoenolpyruvate carboxylase (PEPC) content also increases; this is significant because

in C_3 species PEPC is involved in anaplerotic reactions to replenish the intermediate products of the Krebs cycle, thereby facilitating the synthesis of amino acid precursors [34,35]. However, to date there are few studies of the effect of elevated temperature on *C. quinoa* physiological parameters [3,8]. Some studies report that plant growth and development is not limited by high temperatures (~40 °C), but hot conditions can decrease pollen viability, seed germination, and seed yield [3,8]. High temperatures can increase stomatal conductance, stomatal size, photosynthesis, chlorophyll fluorescence, and chlorophyll content but can also result in reduced water use efficiency [6,9,36]. Moreover, the accumulation of anions and cations in response to high temperatures allows *C. quinoa* to adapt osmotically to overcome increases in the amount of transpired water [10]. Finally, some *C. quinoa* cultivars have a high thermal acclimatization capacity to temperature due to changes in maximum carboxylation capacity (VCmax) of Rubisco [37].

The combined effect of elevated temperature and salinity is an important interaction that frequently reduces agricultural productivity [8,38]. However, to date studies regarding the combined effect of elevated temperatures and salinity on *C. quinoa* are few and inconsistent [6,8,9,39,40]. For example, relative to individual stresses, the combined effect of salinity and elevated temperature reduced the growth of *C. quinoa* and also reduced their grain yield, chlorophyll content, and stomatal conductance [9]. The combined action of elevated temperature and salinity was also found to result in decreased stomatal size and a larger number of EBCs on the abaxial side of *C. quinoa* leaf. This improved the distribution of water and CO_2 and facilitated the proper maintenance of photosynthesis [6]. We hypothesize that the combined effect of elevated temperature and salinity can both exacerbate the effect of individual factors and cause unique plant responses at the level of expression of genes associated with light and dark reactions of photosynthesis and genes that are most sensitive to these stresses. The purpose of this study was to therefore investigate the effects of salinity, elevated temperature, and their interaction on (1) growth and ion–water balance; (2) the efficiency of PSII and activity of CET around PSI; (3) the content of the Rubisco and PEPC enzymes; and (4) expression of photosynthetic genes of *C. quinoa*.

2. Materials and Methods

2.1. Plant Growth Conditions

The quinoa "Vahdat" variety was used in the current study, and the seeds were obtained from the Centre for Genetic Resources of the Tajik Academy of Agricultural Sciences. Seeds of *Chenopodium quinoa* Willd were germinated on filter paper soaked in distilled water within 2–4 days. After that, the seedlings were transplanted to perlite in plastic pots. Each plastic pot was placed on a separate plastic tray. The seedlings were grown over 30 days using the nutrient solution 50% Hoagland, which was added to each plastic tray. The seedlings were grown in two separated climate chambers under circadian illumination (using commercial luminescent white light tubes): 8 h dark/16 h light (200 mmol/(m^2 s) PAR, light meter LI-250A (Li-Cor, Lincoln, NE, USA)), 25 °C and 35 °C temperature. Then half of the plants in both chambers were treated with 300 mM NaCl solution for 4 days.

2.2. Dry Biomass, Water, Ions, and MDA Contents

To determine the dry biomass, the leaves were dried at 80 °C to constant weight. The water content (W) was calculated using the following formula:

$$W = (FW - DW)/DW,$$

where FW is fresh biomass and DW is dry biomass and expressed in g H_2O/g DW.

Na^+ and K^+ contents in the leaves were determined in water extracts on the flame photometer FPA-2-01 (AOOT ZOMZ, Sergiev Posad, Russia). Dry leaves samples (100 mg) from each variant were homogenized in 2 mL of distilled water and heated at 100 °C for

10 min in a water bath, and then the homogenates were centrifuged (5 min, 14,000× *g*). The content of ions was expressed as mmol/g DW.

The rate of lipid peroxidation was assessed spectrophotometrically via a reaction with thiobarbituric acid (TBA), based on the interaction of TBA with malondialdehyde (MDA). The MDA content in leaves was determined as described previously [41]. The weighed, frozen plant leaves (0.20–0.50 g) were ground in a mortar in 2 mL of 0.5% trichloroacetic acid. Homogenate was centrifuged at 10,000× *g* for 10 min, and 0.3 mL of supernatant was mixed with 1.2 mL of solution containing 0.5% (*w*/*v*) thiobarbituric acid and 20% (*w*/*v*) trichloroacetic acid. The mixture was heated in a boiling water bath for 30 min, rapidly cooled on ice, and centrifuged at 10,000× *g* for 10 min. The absorbance of the samples was measured at 532 and 600 nm on the spectrophotometer. The MDA concentration was calculated after subtracting the nonspecific absorbance at 600 nm using the absorption coefficient (155 mM^{-1} cm^{-1}) and was expressed as nmol g/FW.

2.3. Activity of Cyclic Electron Transport of PSI and Efficiency of PSII

The PSI cyclic electron transport activity was measured as the P700 oxidation kinetics in response to far-red illumination by monitoring changes in leaf absorbance as described previously [42]. The quantum yield of PSII fluorescence of a dark-adapted (20 min) leaf was determined using a PAM fluorometer (PAM-101, Heinz-Walz, Effeltrich, Germany). The measurement was carried out with additional illumination of the sample with a weak modulated red light flux, which was carried out by an ADC (PDA-100, Walz, Effeltrich, Germany), which converted the primary signal from the PAM-101 to a computer with a specialized software interface. The calculation of the maximum quantum yield of PSII fluorescence was performed based on the current values of minimal (F_0) and maximal (F_m) fluorescence of a dark-adapted leaf using the following formula:

$$F_v/F_m = (F_m - F_0)/F_m.$$

The maximum quantum efficiency (F'_v/F'_m) of PSII photochemistry at a given light intensity was calculated using the following formula:

$$F'_v/F'_m = (F'_m - F'_0)/F'_m$$

where F'_0 and F'_m are the minimum and maximum chlorophyll fluorescence after light adaptation.

Nonphotochemical quenching of chlorophyll fluorescence (NPQ) was calculated using the following formula:

$$NPQ = (F_m - F'_m)/F'_m.$$

2.4. Western Blot Analysis

Contents of ribulose-1.5-bisphophate carboxylase/oxygenase (Rubisco) and phosphoenolpyruvate carboxylase (PEPC) proteins were determined by means of immunoblotting analysis as described previously [42]. Hybridization was achieved with commercial polyclonal antibodies for proteins of a large subunit (L) of Rubisco at a dilution of 1:10,000 (RbcL, AS03 037, Agrisera, Vännäs, Sweden) and PEPC at a dilution of 1:5000 (AS09 458, Agrisera, Sweden) for 1 h. Immunoreactions were detected using peroxidase-conjugated antirabbit IgG horse radish antibodies (Agrisera, AS09 602). The blots were developed with fluorescent dyes luminol and coumaric acid in the presence of hydrogen peroxide, and signals were visualized by Retina (PRO RETINA, Bonn, Germany). The intensity of Western blotting bands was assessed using ImageJ 1.37v software (NIH, Bethesda, MD, USA) and expressed relative to the average level (n = 3) for control plants, taken as 100%. Equal protein loading was checked by staining of blots with Ponceau. The analysis was repeated at least three times.

2.5. RNA Isolation and Quantitative Real Time (RT)-PCR

Total RNA was extracted from leaf samples (0.50 g FW) by phenol–chloroform extraction with precipitation using LiCl. The concentration of RNA was determined using a NanoDrop 1000 spectrophotometer (Thermo Scientific, MA, USA). RNA was purified from genomic DNA according to the standard ThermoScientific protocol (USA) using DNAse I and RiboLock (ThermoScientific, USA). Reverse transcription was performed according to the standard Evrogen protocol (Evrogen, Moscow, Russia), using (Oligo(dT)15 and Random(dN)10 primers, MMLV reverse transcriptase (Evrogen, Russia), dNTP, and RiboLock (ThermoScientific, USA). The cDNA concentration was measured using a NanoDrop 1000 spectrophotometer (ThermoScientific, USA). PCR primers were designed using Pick Primers NCBI (National Center for Biotechnology Information, Bethesda, MD, USA) with Primer Pair Specificity Checking Parameters and SnapGene Viewer (4.2.11) on nucleotide sequences available in the NCBI database (Table 1). For the study, we chose genes that encode components of proteins and systems involved in photosynthesis and used/measured in this study: Rubisco (*rbcL*) and PEPC (*Ppc1*, *Ppc2*) proteins, PSI (*psaA*, *psaB*) and PSII (*psbA*) components, and components of linear (*FDI*) and cyclic electron transport (*FDII*, *FNR1*, *PGR5*, *NdhH*) (Table 1). The primers were checked, and the amplicon size was determined using PCR (TP4-PCR-01-Tertsik, DNA-Technology, Moscow, Russia) and electrophoresis in 2% agarose gel. The transcripts level was assessed by real-time PCR (RT-qPCR) using a Light Cycler96 amplifier (Roche, Basel, Switzerland) with SybrGreen I dye (Evrogen, Russia). RT-PCR data were analyzed using Light Cycler96 Software Version 1.1. Relative quantification was performed to compare the levels of the target gene and the reference gene, and the result was expressed as a ratio. *UBQ10* and *b-Tubulin* were used as reference genes. Transcript levels were calculated relative to control plants.

Table 1. List of primers.

Primer	Gene	Function	5′–3′ Sequence
rbcL	LOC32958948	Large subunit (L) Rubisco	TCACATGTAGCGGCAGTAGC AGCCGTTTATGCGTTGGAGA
Ppc1	LOC110691154	PEPC isoform 1	GGTTGCTGGGCATAAGGACT ATGCCAGCAGCAATACCCTT
Ppc2	LOC110737782	PEPC isoform 2	GGAGGTGGACCTACCCATCT CTCAAGAGTGGCAGCAGTGA
psaA	LOC32958941	Apoprotein A1 of photosystem I	GTGAGTAGGGTCGCTTAGCC TACCAGCGACTTGGAGGAGA
psaB	LOC32958940	Apoprotein A2 of photosystem I	GAACCGCGTGCATCTAAAGC GCCTGGCTGGTTAAATGCTG
psbA	LOC32959011	Protein D1 of photosystem II	AGACCCGGAAACAGGTTCAC ACCAGCACTGAAAACCGTCT
FDI	LOC110699227	Ferredoxin I protein (a LET participant)	GAGTTTGAGTGCCCGGATGA CTGGTCGAGAGTACCAGACG
FDII	LOC110691003	Ferredoxin II protein (a CET PSI participant)	GAGGGAATGGGGTGGACTTG CTTCAGCCATCTGCCCATCA
FNR1	LOC110694708	Ferredoxin:NADP$^+$ oxidoreductase	TATGCCAACGAACTGTGGGA TCCATTTGCTGCCAGCTTAC
PGR5	LOC110692940	PGR5 protein, a key part of the main CET pathway of PSI	TCACAACCACAAGAGGAGCAA TCGCGTCCGGTGAGAATTAC
NdhH	LOC32959000	49 kDa subunit of the NADH dehydrogenase in the second CET pathway of PSI	GGCCATTTCACCGATTCGTA GGCCCTATGCTACGAGCTTC
UBQ10	LOC110721034	Ubiquitin 10 (reference gene)	CGAGCAGAAACAAGCCTAATCG GCGATTAATTTCCATGTTGTCCG
b-Tubulin	LOC110711758	b-tubulin (reference gene)	ACCGGAGAAGGTATGGACGA GTACTCTTCCTCATCGGCGG

2.6. Statistical Analysis

All analysis were performed using at least three biological replicates. Statistical analyses of data for physiological parameters were performed using SigmaPlot 12.3. The effects of the factors and their interaction were assessed by using two-way ANOVA on analysis platform SigmaPlot 12.5. Mean separation was performed using Normality Test (Shapiro–Wilk) and all Pairwise Multiple Comparison Procedures (Bonferroni *t*-test). Differences were considered significant at $p < 0.05$.

3. Results

3.1. Biomass, Water, Na^+, K^+, and MDA Contents

The shoot length and fresh biomass of *C. quinoa* increased by 1.6-fold and 2.1-fold, respectively, under elevated temperature (Figure 1a,b). The fresh and dry biomass of *C. quinoa* decreased by 1.7-fold under the salinity (300 mM NaCl) treatment and by 3-fold under the combined effect of elevated temperature and salinity (35 °C and 300 mM NaCl) (Figure 1b,c). Under the individual effect of elevated temperature (eTem), the dry biomass remained indistinguishably different from the level of the control plants, whereas the water content increased by almost 2-fold (Figure 1d); Na^+ and K^+ contents increased by 1.7-fold and 2.5-fold, respectively (Figure 1e,f); and the lipid peroxidation level (MDA) increased by 1.6-fold (Figure 1g). At 300 mM NaCl, we observed a fourteenfold increase in sodium ion content in the leaves (Figure 1e). In addition, under the combined effect of elevated temperature and salinity (eTem + NaCl), water content remained at the level of the control plants, whereas K^+ content remained approximately the same as under the individual effect of elevated temperature, and Na^+ content increased by 1.4-fold relative to the individual effect of elevated temperature (Figure 1). Finally, under the eTem + NaCl treatment, we observed a 2.5-fold increase in MDA content relative to control plants and 1.5-fold increase relative to plants grown at 35 °C (Figure 1g, Table 2).

Table 2. Two-way analysis of variance (ANOVA) showing the effect of the salinity and elevated temperature and their interaction) with the growth, photosystems, water, ions and MDA contents, and expression of photosynthetic genes of *Chenopodium quinoa*.

Parameters [1]	MS		
	NaCl	eTem	eTem + NaCl
DW	2.292 ***	0.004	0.310 *
W	5.414	40.897 ***	3.433
Na^+	8.007 ***	4.891 ***	6.344 ***
K^+	0.003	8.103 ***	0.002
MDA	7.993 *	68.260 ***	14.126 **
PSI	1.818	3.367	0.501
F_v/F_m	0.010	0.399 ***	0.013
F'_v/F'_m	0.022	1.021 ***	0.024
rbcL	0.962	4.255 ***	3.895 ***
psbA	4.647	11.706 ***	18.587 ***
FDI	0.012	3.443 ***	3.571 ***
FNR1	2.703 ***	0.604	3.335 ***
PGR5	0.403	0.772	1.751 **

[1] The analysis was carried out for parameters, which were changed under the influence of at least one factor. NaCl—plants grown at 25 °C and treated with 300 mM NaCl over 4 days; eTem—plants grown at 35 °C; eTem + NaCl—plants grown at 35 °C and treated with 300 mM NaCl over 4 days. DW, dry biomass; W, water content; Na^+, sodium content; K^+, potassium content; PSI, activity of PSI CET; F_v/F_m, maximum quantum yield of PSII fluorescence; F'_v/F'_m, maximum quantum efficiency of PSII photochemistry at a given light intensity; *rbcL*, gene encoding the Rubisco large subunit; *psbA*, gene encoding protein D1 of PSII; *FDI*, gene encoding the ferredoxin I protein (a LET participant); *FNR1*, gene encoding the ferredoxin:$NADP^+$ oxidoreductase; *PGR5*, gene encoding PGR5 protein, a key part of the main CET pathway of PSI. * $p < 0.05$, ** $p < 0.01$, *** $p < 0.001$.

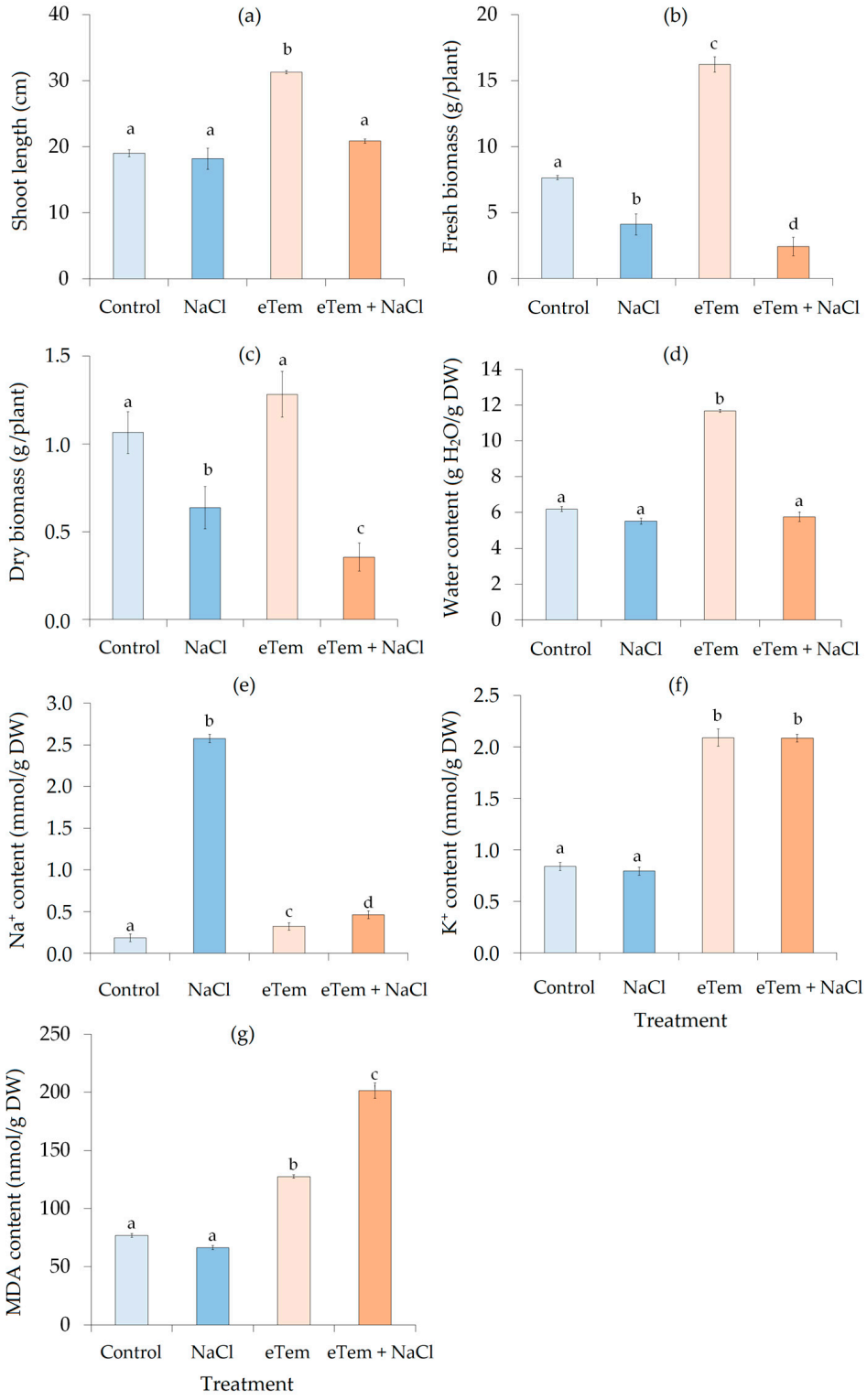

Figure 1. The effect of salinity and elevated temperature, and their interaction with the shoot length (**a**), fresh biomass (**b**), dry biomass (**c**), water (**d**), Na^+ (**e**), K^+ (**f**), and MDA (**g**) contents in leaves of *Chenopodium quinoa*. Control—plants grown at 25 °C without treatment; NaCl—plants grown at 25 °C and treated with 300 mM NaCl over 4 days; eTem—plants grown at 35 °C; eTem + NaCl—plants grown at 35 °C and treated with 300 mM NaCl over 4 days. The different letters show statistically different means at $p \leq 0.05$ (Bonferroni *t*-test).

3.2. Activity of Cyclic Electron Transport for PSI and Efficiency of PSII

We observed that the activity of CET for PSI did not change under any treatment (Figure 2a). Moreover, the maximum quantum efficiency of PSII photochemistry at a given light intensity (F'_v/F'_m) decreased by 50–70% under eTem and eTem + NaCl, which led to a 30–40% decrease in the maximum quantum yield of PSII (F_v/F_m) (Figure 2b,c, Table 2). Finally, the NPQ of chlorophyll fluorescence remained unchanged under all treatments (Figure 2d).

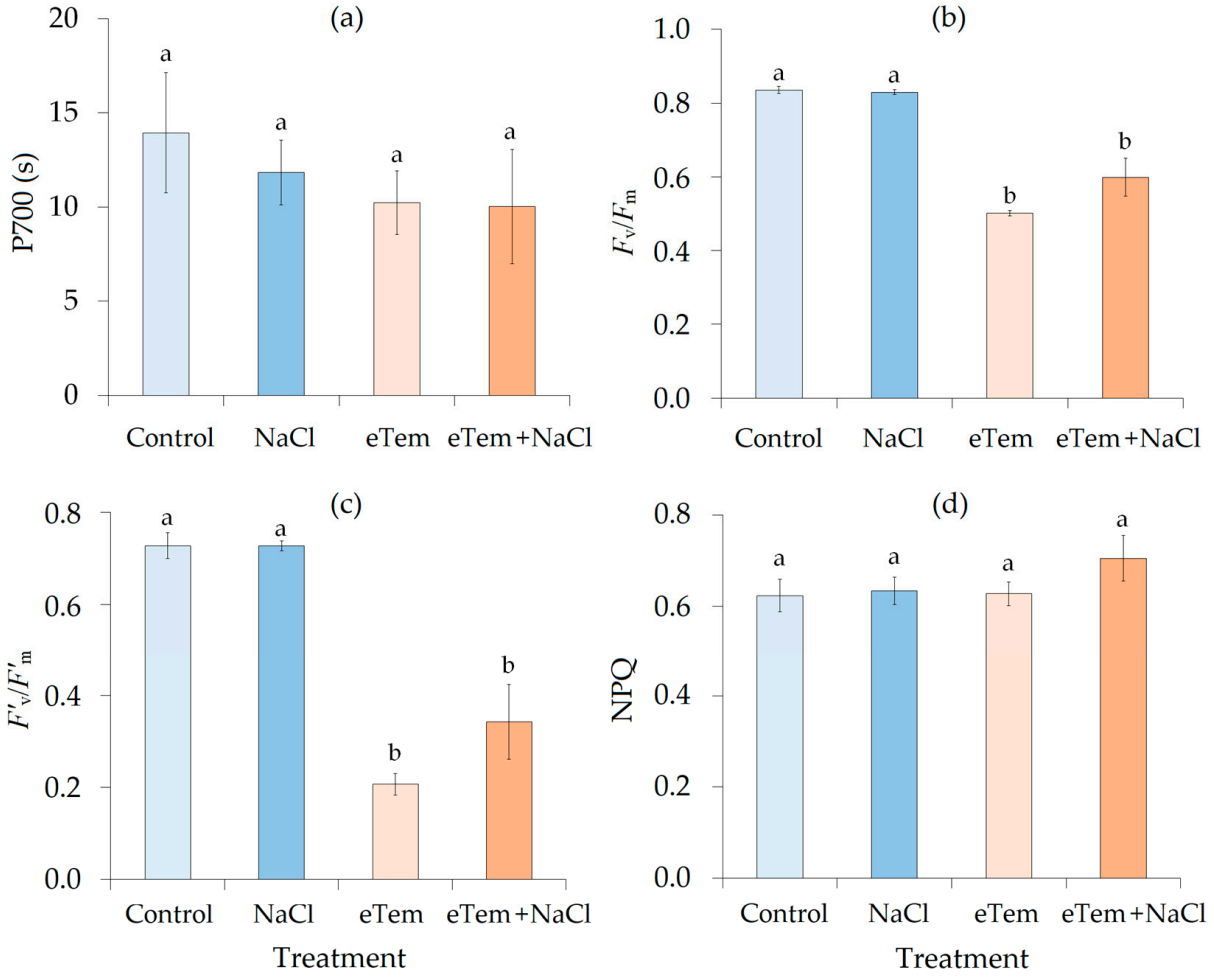

Figure 2. The effect of salinity and elevated temperature, and their interaction with the activity of cyclic electron transport of PSI (**a**), maximum quantum efficiency of PSII (**b**), maximum quantum efficiency of PSII photochemistry at a given light intensity (**c**), and nonphotochemical quenching of chlorophyll fluorescence (**d**) in leaves of *Chenopodium quinoa*. Control—plants grown at 25 °C without treatment; NaCl—plants grown at 25 °C and treated with 300 mM NaCl over 4 days; eTem—plants grown at 35 °C; eTem + NaCl—plants grown at 35 °C and treated with 300 mM NaCl over 4 days. The different letters show statistically different means at $p \leq 0.05$ (Bonferroni *t*-test).

3.3. Western Blot Analysis

No significant changes were observed in Rubisco (large subunit) and PEPC content under any treatment (Figure 3a,b).

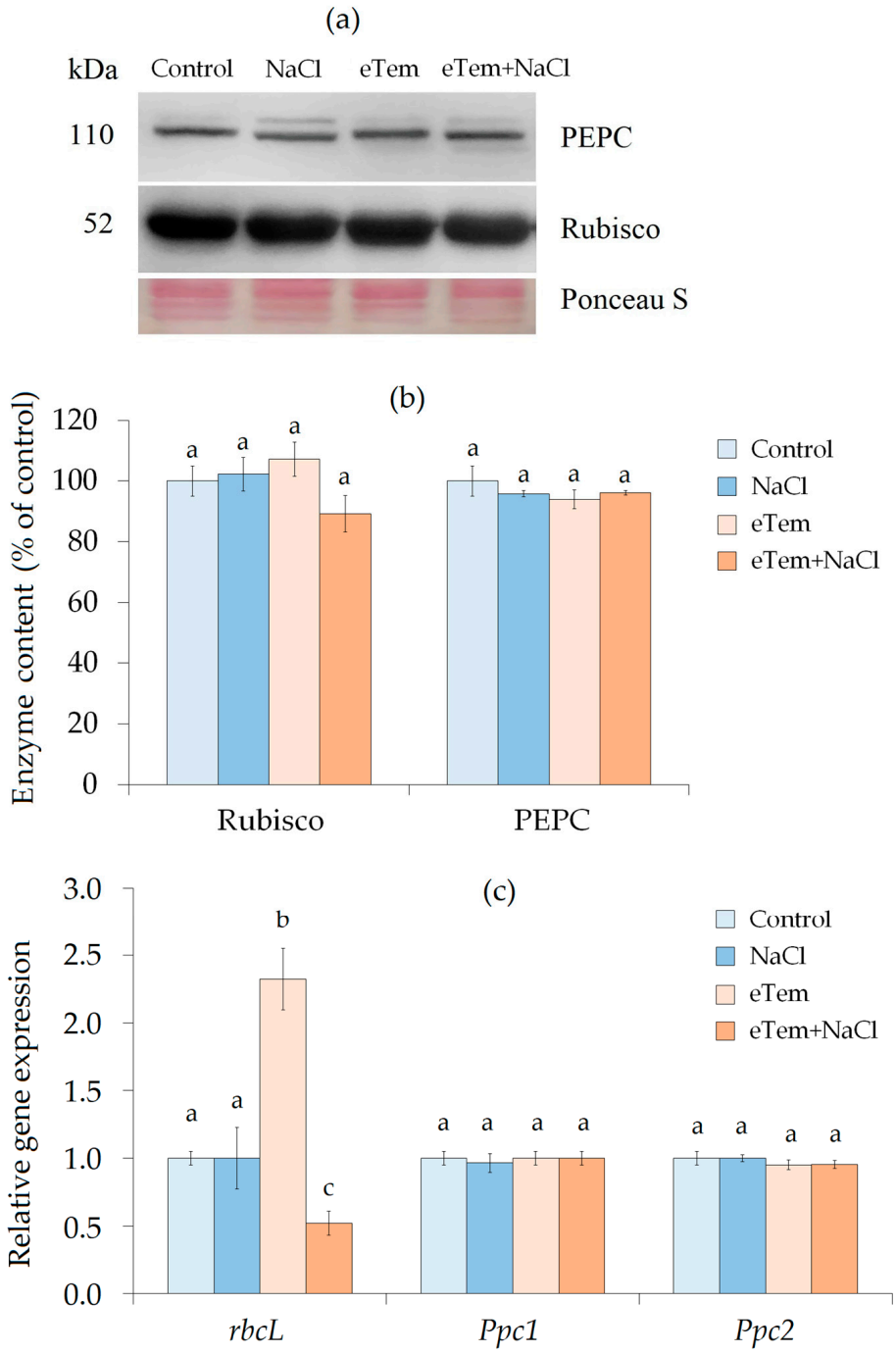

Figure 3. The effect of salinity and elevated temperature, and their interaction with the content of Rubisco and PEPC enzymes (**a**,**b**) and expression of relevant genes (*rbcL*, *Ppc1* and *Ppc2*) (**c**) in leaves of *Chenopodium quinoa*. Blots were probed with antibodies raised against Rubisco (subunit L) and PEPC. Relative enzyme contents are shown on the basis of intensity of Western blotting bands estimated using ImageJ 1.37v software (USA) and expressed relatively to the average level for control plants taken as 100%. Equal protein loading was checked by staining the blots with Ponceau. Control—plants grown at 25 °C without treatment; NaCl—plants grown at 25 °C and treated with 300 mM NaCl over 4 days; eTem—plants grown at 35 °C; eTem + NaCl—plants grown at 35 °C and treated with 300 mM NaCl over 4 days. The different letters show statistically different means at $p \leq 0.05$ (Bonferroni *t*-test).

3.4. Expression of Photosynthetic Genes

Analysis of the expression of genes encoding the Rubisco large subunit (*rbcL*) and PEPC (*Ppc1* and *Ppc2*) revealed changes only in the accumulation of *rbcL* transcripts. Specifically, we observed a 2.3-fold increase under eTem and a 2-fold decrease under eTem + NaCl (Figure 3c). The 300 mM NaCl and eTem treatment did not affect the expression of *psaA* and *psaB*, encoding apoproteins 1 and 2 of PSI (Figure 4). In contrast, elevated temperature upregulated the expression of *psbA*, encoding protein D1 of PSII, whereas eTem + NaCl downregulated *psbA* expression (Figure 4). A similar pattern was observed for the expression of *FDI*, which encodes the ferredoxin I protein (a LET participant). The expression of *FDII*, which encodes the ferredoxin II protein (a CET PSI participant), did not change in response to any treatment (Figure 4). Next, the expression of *FNR1* gene encoding the ferredoxin:$NADP^+$ oxidoreductase (FNR) enzyme was upregulated in response to 300 mM NaCl and was downregulated in response to eTem + NaCl (Figure 4). The combined effect of elevated temperature and salinity also downregulated expression of *PGR5*, which encodes the PGR5 protein, a key part of the main CET pathway of PSI. At the same time, the expression of *NdhH*, which encodes the 49 kDa subunit of the NADH dehydrogenase in the second CET pathway of PSI, remained the same in all treatments (Figure 4). Finally, the significance of the combined effect of elevated temperature and salinity on the expression of *rbcL*, *psbA*, *FDI*, *FNR1*, and *PGR5* was confirmed by a two-way ANOVA (Table 2).

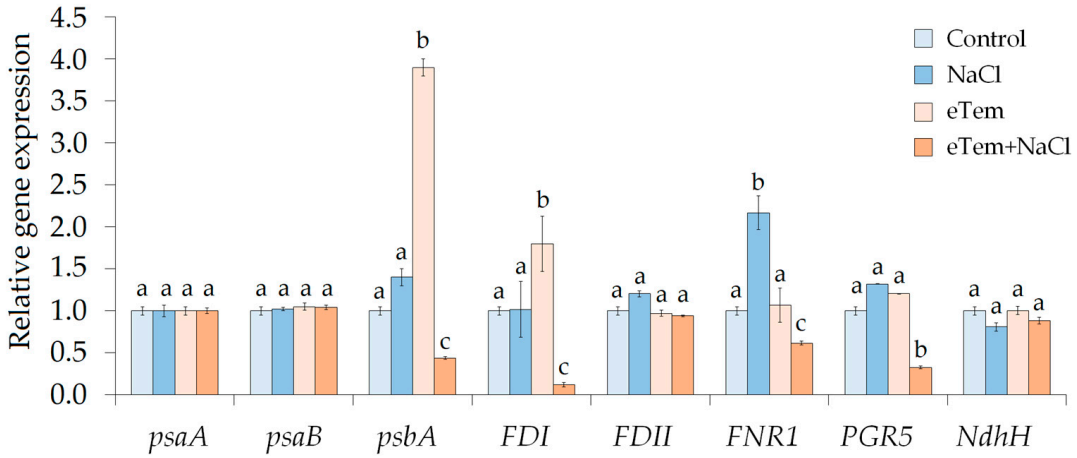

Figure 4. The effect of salinity and elevated temperature, and their interaction with the expression of photosynthetic genes *psaA* and *psaB*, encoding apoproteins 1 and 2 of PSI; *psbA*, encoding protein D1 of PSII; *FDI*, encoding the ferredoxin I protein (a LET participant); *FDII*, encoding the ferredoxin II protein (a CET PSI participant); *FNR1*, gene encoding the ferredoxin:$NADP^+$ oxidoreductase; *PGR5*, gene encoding PGR5 protein of the main CET pathway of PSI; *NdhH*, encoding the 49 kDa subunit of the NADH dehydrogenase in the second CET of PSI in leaves of *Chenopodium quinoa*. Control—plants grown at 25 °C without treatment; NaCl—plants grown at 25 °C and treated with 300 mM NaCl over 4 days; eTem—plants grown at 35 °C; eTem + NaCl—plants grown at 35 °C and treated with 300 mM NaCl over 4 days. The different letters show statistically different means at $p \leq 0.05$ (Bonferroni *t*-test) between treatments for each gene separately.

4. Discussion

The salinity conditions for optimal growth of *C. quinoa* (a halophyte) are between 100 and 200 mM NaCl [8], and a significant decrease in the biomass begins to occur at 300–400 mM NaCl [13,43]. However, a decrease in the biomass of some *C. quinoa* varieties was observed even at 100–200 mM NaCl [6,44]. In our experiment, the 300 mM NaCl treatment led to an almost twofold decrease in *C. quinoa* biomass (Figure 1). In this case, *C. quinoa* accumulated significant amount of Na^+, which is used as a cheap osmolyte by halophytes [45]. However, in *C. quinoa*, no negative effect of ionic stress was observed on

the efficiency of PSII, the activity of LET and CET, or the expression of the corresponding genes, except for *FNR1*. In higher plants, several isoforms (1–3) of the FNR enzyme have been identified. This enzyme catalyzes $NADP^+$ reduction at the final stage of LET and also participates in the CET in PSI [46,47]. Moreover, it may be accumulated in excess under salt stress [48]. We also found that the content of Rubisco and PEPC enzymes and the transcription levels of their corresponding genes, i.e., *rbcL*, *Ppc1*, and *Ppc2*, did not change in response to salinity stress (Figure 3). This may be due to the short period of salinity exposure in this experiment, and a longer exposure to 300 mM NaCl could result in a decrease in the activity of photosynthetic enzymes and the efficiency of PSII [13,16,18]. Low MDA content indicates the absence of significant lipid peroxidation and, consequently, oxidative stress (Figure 1d). Perhaps, the decrease in *C. quinoa* biomass is a consequence of the osmotic component of salinity, which in turn causes a decrease in stomatal conductivity. This can lead to a reduction in water loss by the plant, but since CO_2 uptake is reduced at the same time, this process can lead to photosynthesis suppression [8,16].

We note that elevated temperature did not affect dry biomass accumulation of *C. quinoa* in our experiment; this finding is consistent with those of other studies [10]. Here, elevated temperature led to increased leaf hydration and cation uptake. We observed an increase in the sum of cations of 2.5 times (Figure 1), and this allowed plants to osmotically adapt to the increase in transpiration accompanying high temperatures [10]. Potassium, which plays an important role in resistance to thermal stress [49], was accumulated to a greater extent in *C. quinoa* than Na^+ (Figure 1). K^+ also participates in ion homeostasis stabilization, can act as an osmolyte, and helps maintain stomatal conductance [50], despite the fact that Na^+ and Cl^- are the main osmolytes used by halophytes [45]. Elevated temperatures often lead to a decrease in PSII efficiency [19,22]; however, in our experiment, a decrease in maximum PSII quantum yield was associated with a significant decrease in F'_v/F'_m, and no enhancement of NPQ of chlorophyll fluorescence was observed (Figure 2). This may be due to the degradation of the D1 protein, which is considered to be the most sensitive component of PSII [19,51]. A significant increase in *psbA* expression (i.e., the gene that codes for the D1 protein) may also be a response to decreased D1 protein content. In addition, elevated temperatures also upregulate *FDI*, which encodes ferredoxin I (Fd I), a key protein involved in LET [27]. The negative effect of elevated temperature on PSII efficiency may be result of oxidative stress [19], as evidenced by increased MDA levels (Figure 1). However, elevated temperature did not have any effect on CET activity or on the expression of genes associated with CET and PSI. Furthermore, the stability of PSI A/B protein levels under moderate heat has also been reported for other species [52]. Here, elevated temperatures caused an increase in *rbcL* expression in *C. quinoa*, but no change in Rubisco enzyme content was observed (Figure 3). The disproportion between *rbcL* transcript content and Rubisco enzyme content may be a consequence of post-transcriptional regulation [53]. In addition, it is possible that Rubisco protein degradation processes were enhanced by stress conditions [33]. Thus, elevated temperatures stimulated the uptake of potassium ions in *C. quinoa*, probably to act as an osmolyte and to maintain water balance when sodium is deficient. Finally, elevated temperature negatively affected PSII efficiency but upregulated the expression of genes encoding components of PSII (*psbA*) and LET (*FDI*), as well as Rubisco (*rbcL*), the main photosynthetic protein.

Importantly, the combined effect of elevated temperature and salinity stress led to a greater decrease in *C. quinoa* biomass than was observed in response to salinity alone (Figure 1). A decrease in the water content of leaves relative to the individual temperature effect indicates that osmotic stress was caused by salinity. Moreover, the Na^+ content of leaves increased by only 40% under eTem + NaCl compared with the eTem treatment, and this was 5.5-fold lower than under the individual effect of salinity (Figure 1). This may be due to the high level of potassium in plant tissues, which at elevated temperatures can play a more important role in adaptation to salinity, as has been shown for the halophyte *K. prostrata* [54]. At the same time, eTem + NaCl did not worsen the negative effect on PSII function or Rubisco and PEPC enzyme content compared to the eTem treatment. Moreover,

the eTem + NaCl treatment radically changed the expression patterns of genes encoding the components of PSII, LET, and Rubisco. We found that the expression of *psbA*, *FDI*, and *rbcL* was downregulated, which contrasts with the upregulation seen in response to the elevated temperature treatment. Changes in the expression of photosynthetic genes reflect the metabolic state of chloroplasts [53,55], which are assessed by oxidative and reductive signaling pathways that regulate gene transcription and post-transcriptional processing [56]. Here, the activity of CET for PSI and the expression of *psaA* and *psaB* (which code for apoproteins A and B of PSI), *FDII* (which codes for the CET protein Fd II), and *NdhH* (which codes for protein NDH-dependent CET) remained unchanged (Figure 4). However, expression of *FNR1* and *PGR5*, which encode the FNR and PGR5 proteins, respectively, was downregulated by eTem + NaCl. In Arabidopsis, the relationship between the proteins involved in CET for PSI has already been shown and involves FNR, PGRL1 (i.e., a participant in PGR5/PGRL1-dependent CET), Fd, PsaD (i.e., a PSI-D subunit), and Cytb6 [57]. The similar expression response of *FNR1* and *PGR5* suggests that the *FNR1* gene in *C. quinoa* encodes the FNR isoform that is involved in CET. In tomato plants subjected to high temperature treatments, it has been shown that inhibition of PGR5/PGRL1-dependent CET disrupts the ROS uptake system, which leads to ROS accumulation [22,24] and consequently increases oxidative stress. In *C. quinoa*, the combined effect of eTem + NaCl did cause significant oxidative stress (Figure 1), and this may be associated with the osmotic component of salinity and a possible decrease in PGR5/PGRL1-dependent CET of PSI. In tobacco, it has been shown that the NDH-dependent pathway plays a critical role in CET of PSI at high temperatures [29,31]. NDH-dependent CET of PSI is involved in ATP supply when ATP demand is high, as occurs in response to high temperature or osmotic stress [29,58]. Thus, the combined effect of elevated temperature and salinity on *C. quinoa* plants in a similar manner downregulated genes encoding the main photosynthetic enzyme (*rbcL*), the most sensitive component of PSII protein D1 (*psbA*), a participant in the LET (*FDI*), which can lead to functional changes in carboxylation and LET. Finally, a decrease in *PGR5* gene expression may cause a change in the role of PGR5/PGRL1-dependent CET pathway in favor of the NDH-dependent CET pathway of PSI.

5. Conclusions

C. quinoa is a salt-tolerant crop that has adapted to a wide range of marginal agricultural soils, as well as high salinity and various temperature conditions. Our results showed that decreases in the biomass under 300 mM NaCl salinity were probably due to stomatal limitations since no metabolic limitations on photosynthesis or changes in photosynthetic gene expression were observed. Under elevated temperatures, the decrease in PSII efficiency was accompanied by upregulation of genes encoding the components of PSII (*psbA*) and LET (*FDI*), as well as the main photosynthetic protein Rubisco (*rbcL*). The combined effect of elevated temperature and salinity caused significant oxidative stress, which led to significant decrease in the biomass and PSII efficiency, as well as downregulation of *psbA*, *FDI*, and *rbcL*. Significant fluctuations in transcript accumulation of these genes indicate that their expression is sensitive to elevated temperature and to the combination of elevated temperature and salt stress in *C. quinoa*. Significant differences in the plant response even to short-term salinity at different temperatures indicate the necessity for further study of the role of expression of genes encoding the linear and cyclic electron transport components under the combined effect of several factors in longer experiments. An in-depth research into the contribution of PGR5/PGRL1-dependent and NDH-dependent pathways and their relationship with the activity of CET of PSI during photosynthesis is also recommended, as it may provide new strategies for increasing the yield of this crop under conditions of multifactorial stresses and/or climate change.

Author Contributions: Conceptualization, E.S. and Z.R.; methodology, E.S., Z.R. and M.P.; software, E.S., M.P. and V.K.; validation, E.S., Z.R. and M.P.; formal analysis, E.S.; investigation, E.S., Z.R., M.P., V.K. and N.L.; resources, E.S. and V.K.; data curation, E.S.; writing—original draft preparation, E.S.; writing—review and editing, Z.R. and M.P.; visualization, M.P. and N.L.; supervision, Z.R.; project administration, M.P.; funding acquisition, Z.R. All authors have read and agreed to the published version of the manuscript.

Funding: This research was funded by the state assignment of Ministry of Science and Higher Education of the Russian Federation (theme no. 122042700044-6) and within RFBR grant (No. 21-54-50006).

Institutional Review Board Statement: Not applicable.

Data Availability Statement: Not applicable.

Conflicts of Interest: The authors declare no conflict of interest.

References

1. Basu, S.; Kumar, A.; Benazir, I.; Kumar, G. Reassessing the role of ion homeostasis for improving salinity tolerance in crop plants. *Physiol. Plant.* **2021**, *171*, 502–519. [CrossRef]
2. Ivushkin, K.; Bartholomeus, H.; Bregt, A.K.; Pulatov, A.; Kempen, B.; De Sousa, L. Global mapping of soil salinity change. *Remote Sens. Environ.* **2019**, *231*, 111260. [CrossRef]
3. Shabala, S. Learning from halophytes: Physiological basis and strategies to improve abiotic stress tolerance in crops. *Ann. Bot.* **2013**, *112*, 1209–1221. [CrossRef]
4. Solomon, B.D. Intergovernmental panel on climate change (IPCC). In *Dictionary of Ecological Economics*; Edward Elgar Publishing: Cheltenham, UK, 2023; p. 302. [CrossRef]
5. Wahid, A.; Gelani, S.; Ashraf, M.; Foolad, M.R. Heat tolerance in plants: An overview. *Environ. Exp. Bot.* **2007**, *61*, 199–223. [CrossRef]
6. Becker, V.I.; Goessling, J.W.; Duarte, B.; Caçador, I.; Liu, F.; Rosenqvist, E.; Jacobsen, S.-E. Combined effects of soil salinity and high temperature on photosynthesis and growth of quinoa plants (*Chenopodium quinoa*). *Funct. Plant Biol.* **2017**, *44*, 665–678. [CrossRef] [PubMed]
7. Toderich, K.N.; Mamadrahimov, A.A.; Khaitov, B.B.; Karimov, A.A.; Soliev, A.A.; Nanduri, K.R.; Shuyskaya, E.V. Differential Impact of Salinity Stress on Seeds Minerals, Storage Proteins, Fatty Acids, and Squalene Composition of New Quinoa Genotype, Grown in Hyper-Arid Desert Environments. *Front. Plant Sci.* **2020**, *11*, 607102. [CrossRef] [PubMed]
8. Hinojosa, L.; González, J.A.; Barrios-Masias, F.H.; Fuentes, F.; Murphy, K.M. Quinoa Abiotic Stress Responses: A Review. *Plants* **2018**, *7*, 106. [CrossRef]
9. Abbas, G.; Areej, F.; Asad, S.A.; Saqib, M.; Anwar-ul-Haq, M.; Afzal, S.; Murtaza, B.; Amjad, M.; Naeem, M.A.; Akram, M.; et al. Differential Effect of Heat Stress on Drought and Salt Tolerance Potential of Quinoa Genotypes: A Physiological and Biochemical Investigation. *Plants* **2023**, *12*, 774. [CrossRef] [PubMed]
10. Yang, A.; Akhtar, S.S.; Amjad, M.; Iqbal, S.; Jacobsen, S.-E. Growth and physiological responses of quinoa to drought and temperature stress. *J. Agron. Crop Sci.* **2016**, *202*, 445–453. [CrossRef]
11. Ruiz, K.B.; Rapparini, F.; Bertazza, G.; Silva, H.; Torrigiani, P.; Biondi, S. Comparing salt-induced responses at the transcript level in a salares and coastal-lowlands landrace of quinoa (*Chenopodium quinoa* Willd). *Environ. Exp. Bot.* **2017**, *139*, 127–142. [CrossRef]
12. Orsini, F.; Accorsi, M.; Gianquinto, G.; Dinelli, G.; Antognoni, F.; Carrasco, K.B.R.; Martinez, E.A.; Alnayef, M.; Marotti, I.; Bosi, S.; et al. Beyond the ionic and osmotic response to salinity in *Chenopodium quinoa*: Functional elements of successful halophytism. *Funct. Plant Biol.* **2011**, *38*, 818–831. [CrossRef]
13. Manaa, A.; Goussi, R.; Derbali, W.; Cantamessa, S.; Abdelly, C.; Barbato, R. Salinity tolerance of quinoa (*Chenopodium quinoa* Willd) as assessed by chloroplast ultrastructure and photosynthetic performance. *Environ. Exp. Bot.* **2019**, *162*, 103–114. [CrossRef]
14. Waqas, M.; Yaning, C.; Iqbal, H.; Shareef, M.; ur Rehman, H.; Bilal, H.M. Synergistic consequences of salinity and potassium deficiency in quinoa: Linking with stomatal patterning, ionic relations and oxidative metabolism. *Plant Physiol. Biochem.* **2021**, *159*, 17–27. [CrossRef]
15. Shabala, L.; Mackay, A.; Tian, Y.; Jacobsen, S.E.; Zhou, D.; Shabala, S. Oxidative stress protection and stomatal patterning as components of salinity tolerance mechanism in quinoa (*Chenopodium quinoa*). *Physiol. Plant.* **2012**, *146*, 26–38. [CrossRef]
16. Delatorre-Herrera, J.; Ruiz, K.B.; Pinto, M. The Importance of Non-Diffusional Factors in Determining Photosynthesis of Two Contrasting Quinoa Ecotypes (*Chenopodium quinoa* Willd.) Subjected to Salinity Conditions. *Plants* **2021**, *10*, 927. [CrossRef] [PubMed]
17. Razzaghi, F.; Jacobsen, S.-E.; Jensen, C.R.; Andersen, M.N. Ionic and photosynthetic homeostasis in quinoa challenged by salinity and drought—Mechanisms of tolerance. *Funct. Plant Biol.* **2014**, *42*, 136–148. [CrossRef] [PubMed]
18. Killi, D.; Haworth, M. Diffusive and Metabolic Constraints to Photosynthesis in Quinoa during Drought and Salt Stress. *Plants* **2017**, *6*, 49. [CrossRef] [PubMed]

19. Allakhverdiev, S.I.; Kreslavski, V.D.; Fomina, I.R.; Los, D.A.; Klimov, V.V.; Mimuro, M.; Mohanty, P.; Carpentier, R. Inactivation and Repair of Photosynthetic Machinery under Heat Stress. In *Photosynthesis: Overviews on Recent Progress and Future Perspective*; IK International Publishing House Pvt. Ltd.: New Delhi, India, 2012; p. 189.
20. Almeselmani, M.; Deshmukh, P.S.; Chinnusamy, V. Effects of prolonged high temperature stress on respiration, photosynthesis and gene expression in wheat (*Triticum aestivum* L.) varieties differing in their thermotolerance. *Plant Stress* **2012**, *6*, 25–32.
21. Muhammad, I.; Shalmani, A.; Ali, M.; Yang, Q.-H.; Ahmad, H.; Li, F.B. Mechanisms Regulating the Dynamics of Photosynthesis Under Abiotic Stresses. *Front. Plant Sci.* **2021**, *11*, 615942. [CrossRef]
22. Yanhui, C.; Hongrui, W.; Beining, Z.; Shixing, G.; Zihan, W.; Yue, W.; Huihui, Z.; Guangyu, S. Elevated air temperature damage to photosynthetic apparatus alleviated by enhanced cyclic electron flow around photosystem I in tobacco leaves. *Ecotoxicol. Environ. Saf.* **2020**, *204*, 111136. [CrossRef]
23. Fan, D.Y.; Fitzpatrick, D.; Oguchi, R.; Ma, W.; Kou, J.; Chow, W.S. Obstacles in the quantification of the cyclic electron flux around photosystem I in leaves of C_3 plants. *Photosynth. Res.* **2016**, *129*, 239–251. [CrossRef]
24. Lu, J.; Yin, Z.; Lu, T.; Yang, X.; Wang, F.; Qi, M.; Li, T.; Liu, Y. Cyclic electron flow modulate the linear electron flow and reactive oxygen species in tomato leaves under high temperature. *Plant Sci.* **2020**, *292*, 110387. [CrossRef]
25. Sonoike, K. Photoinhibition of photosystem I. *Physiol. Plant.* **2011**, *142*, 56–64. [CrossRef]
26. Munekage, Y.; Hashimoto, M.; Miyake, C.; Tomizawa, K.I.; Endo, T.; Tasaka, M.; Shikanai, T. Cyclic electron flow around photosystem I is essential for photosynthesis. *Nature* **2004**, *429*, 579–582. [CrossRef] [PubMed]
27. Shikanai, T. Cyclic electron transport around photosystem I: Genetic approaches. *Annu. Rev. Plant Biol.* **2007**, *58*, 199–217. [CrossRef] [PubMed]
28. Yamori, W.; Shikanai, T. Physiological functions of cyclic electron transport around photosystem I in sustaining photosynthesis and plant growth. *Annu. Rev. Plant Biol.* **2016**, *67*, 81–106. [CrossRef] [PubMed]
29. Ma, M.; Liu, Y.; Bai, C.; Yang, Y.; Sun, Z.; Liu, X.; Zhang, S.; Han, X.; Yong, J.W.H. The Physiological Functionality of PGR5/PGRL1-Dependent Cyclic Electron Transport in Sustaining Photosynthesis. *Front. Plant Sci.* **2021**, *12*, 702196. [CrossRef]
30. Shikanai, T.; Yamamoto, H. Contribution of cyclic and pseudo-cyclic electron transport to the formation of proton motive force in chloroplasts. *Mol. Plant* **2017**, *10*, 20–29. [CrossRef]
31. Wang, P.; Duan, W.; Takabayashi, A.; Endo, T.; Mi, H. Chloroplastic NAD(P)H dehydrogenase in tobacco leaves functions in alleviation of oxidative damage caused by temperature stress. *Plant Physiol.* **2006**, *141*, 465–474. [CrossRef]
32. He, Y.; Yu, C.; Zhou, L.; Chen, Y.; Liu, A.; Jin, J.; Hong, J.; Qi, Y.; Jiang, D. Rubisco decrease is involved in chloroplast protrusion and Rubisco-containing body formation in soybean (*Glycine max*.) under salt stress. *Plant Physiol. Biochem.* **2014**, *74*, 118–124. [CrossRef]
33. Yoshitake, Y.; Nakamura, S.; Shinozaki, D.; Izumi, M.; Yoshimoto, K.; Ohta, H.; Shimojima, M. RCB-mediated chlorophagy caused by oversupply of nitrogen suppresses phosphate-starvation stress in plants. *Plant Physiol.* **2021**, *185*, 318–330. [CrossRef] [PubMed]
34. Jeanneau, M.; Vidal, J.; Gousset-Dupont, A.; Lebouteiller, B.; Hodges, M.; Gerentes, D.; Perez, P. Manipulating PEPC levels in plants. *J. Exp. Bot.* **2002**, *53*, 1837–1845. [CrossRef] [PubMed]
35. O'Leary, B.; Park, J.; Plaxton, W.C. The remarkable diversity of plant PEPC (phosphoenolpyruvate carboxylase): Recent insights into the physiological functions and post-translational controls of non-photosynthetic PEPCs. *Biochem. J.* **2011**, *436*, 15–34. [CrossRef] [PubMed]
36. Eustis, A.; Murphy, K.M.; Barrios-Masias, F.H. Leaf Gas Exchange Performance of Ten Quinoa Genotypes under a Simulated HeatWave. *Plants* **2020**, *9*, 81. [CrossRef] [PubMed]
37. Bunce, J. Thermal acclimation of the temperature dependence of the V_{Cmax} of Rubisco in quinoa. *Photosynthetica* **2018**, *56*, 1171–1176. [CrossRef]
38. Mittler, R. Abiotic stress, the field environment and stress combination. *Trends Plant Sci.* **2006**, *11*, 15–19. [CrossRef]
39. Hinojosa, L.; Matanguihan, J.B.; Murphy, K.M. Effect of high temperature on pollen morphology, plant growth and seed yield in quinoa (*Chenopodium quinoa* Willd.). *J. Agron. Crop Sci.* **2019**, *205*, 33–45. [CrossRef]
40. Mamedi, A.; Afshari, R.T.; Sepahvand, N.A.; Oweyse, M. Evaluation of various temperatures on *Quinoa* plant seeds under salinity stress. *Iran. J. Field Crop Sci.* **2016**, *46*, Pe583–Pe589.
41. Voronin, P.Y.; Maevskaya, S.N.; Nikolaeva, M.K. Physiological and molecular responses (*Zea mays* L.) plants to drought and rehydration. *Photosynthetica* **2019**, *57*, 850–856. [CrossRef]
42. Shuyskaya, E.; Rakhmankulova, Z.; Prokofieva, M.; Saidova, L.; Toderich, K.; Voronin, P. Intensity and duration of salinity required to form adaptive response in C_4 halophyte *Kochia prostrata* (L.) Shrad. *Front. Plant Sci.* **2022**, *13*, 955880. [CrossRef]
43. Eisa, S.; Hussin, S.; Geissler, N.; Koyro, H.W. Effect of NaCl salinity on water relations, photosynthesis and chemical composition of Quinoa (*Chenopodium quinoa* Willd.) as a potential cash crop halophyte. *Aust. J. Crop Sci.* **2012**, *6*, 357–368.
44. Talebnejad, R.; Sepaskhah, A.R. Physiological characteristics, gas exchange, and plant ion relations of quinoa to different saline groundwater depths and water salinity. *Arch. Agron. Soil Sci.* **2016**, *62*, 1347–1367. [CrossRef]
45. Flowers, T.J.; Glenn, E.P.; Volkov, V. Could vesicular transport of Na^+ and Cl^- be a feature of salt tolerance in halophytes? *Ann. Bot.* **2019**, *123*, 1–18. [CrossRef] [PubMed]

46. Okutani, S.; Hanke, G.T.; Satomi, Y.; Takao, T.; Kurisu, G.; Suzuki, A.; Hase, T. Three Maize Leaf Ferredoxin: NADPH Oxidoreductases Vary in Subchloroplast Location, Expression, and Interaction with Ferredoxin. *Plant Physiol.* **2005**, *139*, 1451–1459. [CrossRef] [PubMed]
47. Mulo, P. Chloroplast-targeted ferredoxin-NADP(+) oxidoreductase (FNR): Structure, function and location. *Biochim. Biophys. Acta Bioenerg.* **2011**, *1807*, 927–934. [CrossRef] [PubMed]
48. Zörb, C.; Herbst, R.; Forreiter, C.; Schubert, S. Short-term effects of salt exposure on the maize chloroplast protein pattern. *Proteomics* **2009**, *9*, 4209–4220. [CrossRef] [PubMed]
49. Hasanuzzaman, M.; Bhuyan, M.H.M.B.; Nahar, K.; Hossain, M.S.; Al Mahmud, J.; Hossen, M.S.; Masud, A.A.C.; Moumita; Fujita, M. Potassium: A vital regulator of plant responses and tolerance to abiotic stresses. *Agronomy* **2018**, *8*, 31. [CrossRef]
50. Azedo-Silva, J.; Osorio, J.; Fonseca, F.; Correia, M.J. Effects of soil drying and subsequent rewatering on the activity of nitrate reductase in roots and leaves of *Helianthus annuus*. *Funct. Plant Biol.* **2004**, *31*, 611–621. [CrossRef]
51. Wen, X.; Qiu, N.; Lu, Q.; Lu, C. Enhanced thermotolerance of photosystem II in salt-adapted plants of the halophyte *Artemisia anethifolia*. *Planta* **2005**, *220*, 486–497. [CrossRef]
52. Quiles, M.J. Stimulation of chlororespiration by heat and high light intensity in oat plants. *Plant Cell Environ.* **2006**, *29*, 1463–1470. [CrossRef]
53. Kusnetsov, V.V. Chloroplasts: Structure and Expression of the Plastid Genome. *Russ. J. Plant Physiol.* **2018**, *65*, 465–476. [CrossRef]
54. Rakhmankulova, Z.F.; Shuyskaya, E.V.; Prokofieva, M.Y.; Toderich, K.N.; Yamanaka, N.; Voronin, P.Y. The effect of elevated temperature on salt tolerance mechanism in C_4 xero-halophyte *Kochia prostrata*. *Russ. J. Plant Physiol.* **2022**, *69*, 137. [CrossRef]
55. Foyer, C.H.; Neukermans, J.; Queval, G.; Noctor, G.; Harbinson, J. Photosynthetic control of electron transport and the regulation of gene expression. *J. Exp. Bot.* **2012**, *63*, 1637–1661. [CrossRef] [PubMed]
56. Pfannschmidt, T.; Liere, K. Redox regulation and modification of proteins controlling chloroplast gene expression. *Antioxid. Redox Signal.* **2005**, *7*, 607–618. [CrossRef] [PubMed]
57. DalCorso, G.; Pesaresi, P.; Masiero, S.; Aseeva, E.; Schunemann, D.; Finazzi, G.; Joliot, P.; Barbato, R.; Leister, D. A complex containing PGRL1 and PGR5 is involved in the switch between linear and cyclic electron flow in Arabidopsis. *Cell* **2008**, *132*, 273–285. [CrossRef] [PubMed]
58. Rumeau, D.; Peltier, G.; Cournac, L. Chlororespiration and cyclic electron flow around PSI during photosynthesis and plant stress response. *Plant Cell Environ.* **2007**, *30*, 1041–1051. [CrossRef]